

## **Role of Grain-boundary-free Energy & Surface-free Energy for Tin Whisker Growth**

*Kiyotaka Tsuji, Research and Development Department,  
Ishihara Chemical Co., Ltd., Kobe, Japan*

The grain-boundary-free energy of tin electrodeposits has been estimated by determining the grain sizes as a function of the thickness. Then the morphology of various whiskers, including the fractured section of their roots, and so-called nodules, which are the irregularly shaped mass-extrusion from the tin surface, has been studied. It has been shown that the grain-boundary-free energy is sufficient for spontaneous occurrence of recrystallization of the layer, especially in the case of thin layers because of their extremely small grains. While many whiskers were found to grow on nodules, this means many whiskers were not formed directly on/in the tin layers. From these facts, it has been suggested that the nodule formation can be explained by recrystallization, and the whisker growth can be understood as a result of minimization of the surface-free energy of nodules, which have large surface-free energy as a result of their complicated surfaces.

**For more information, contact:**

Kiyotaka Tsuji  
R & D Department  
Ishihara Chemical Co., Ltd.  
5-26, Nishi-yanagihara-cho,  
Hyogo-ku, Kobe 652-0806, Japan  
Tel: 81-78-682-2322  
Fax: 81-78-682-4513  
E-mail: tsuji-k@unicon.co.jp

## 1. Introduction

It is well known that filamentary shaped whiskers grow spontaneously from electrodeposited tin layers at room temperature. The tin whiskers show unique property, e.g. they consist of single crystals of  $\beta$ -tin growing in several specific directions<sup>1, 2</sup> and include an extremely small number of dislocations<sup>3</sup>. Their cross sectional shapes are constant throughout almost whole length. Stored strain energy in deposits<sup>4, 5</sup> or compressive stress, induced by formation of intermetallic compound at the interface between deposits and substrates<sup>6, 7</sup>, were considered to be the driving force for the whisker growth. Regarding growth mechanism of whiskers, several models were proposed. J. D. Eshelby<sup>8</sup>, F. C. Franc<sup>9</sup>, U. Lindborg<sup>10</sup>, and B. Z. Lee et al.<sup>7</sup> attempted to explain the whisker growth by dislocation movement. While, W. C. Ellis et al.<sup>11</sup>, and N. Furuta et al.<sup>12</sup> proposed the models based on recrystallization. However we have not yet achieved complete understanding of this peculiar phenomenon at the present.

Generally the grain sizes of electrodeposited tin layers are extremely smaller than that of bulk material. Therefore grain-boundary-free energy of the deposits is expected to act as the driving force of the whisker growth. In this work, to reveal the roll of the grain-boundary-free energy on whisker growth, it has been estimated by determining the grain sizes as a function of the thickness. Then the morphology of various whiskers, including the fractured section of their roots, and so-called nodules, which are the irregularly shaped mass-extrusion from the tin surface, has been studied to understand whisker growth process in detail. If the dimension of a structure is sufficiently small like whiskers, the tendency to lower its surface-free energy is the principal motivation for changes in structures<sup>13</sup>. From this perspective, we have discussed whisker growth mechanism.

## 2. Experimental Procedure

### 2.1 Electrodeposition of Specimen

Three different types of plating solution, shown in Table 1, were used for preparing specimens for observation of whiskers and nodules. Matt Sn, bright Sn and matt Sn-0.5%Cu were electrodeposited on copper substrate. (Percent in this paper means mass percent, unless otherwise stated.) Matt Sn-0.5%Cu was used for acceleration of the whisker growth as reported in literatures<sup>14, 15</sup>. The thickness of the deposits was measured with an X-ray fluorescent coating thickness gauge. The specimens were stored at room temperature and 100 °C to grow whiskers and nodules for 751 days at maximum.

### 2.2 Determination of Grain Size

The grain sizes were determined as a function of the thickness of deposits. For matt Sn and matt Sn-0.5%Cu, a line of certain length  $l$  was drawn arbitrarily on the scanning electron microscope (SEM) image of grains, and the number  $n$  of the grains located on the line was counted. Then  $l/n$  gives the average grain size  $d$ . For bright Sn, specimens were etched with an aqueous solution of 100 g/L ammonium persulfate prior to the determination of grain sizes because the grains were not recognized apparently.

Table 1 Composition of plating solution and plating conditions.

Items	Matt Sn	Bright Sn	Matt Sn-0.5%Cu
Sn <sup>2+</sup> (g/L)*	20	20	59.3
Cu <sup>2+</sup> (g/L)**			0.75
Free Acid (g/L)***	100	100	140
Additive	Additives commercially provided were used.		
Current density (A/dm <sup>2</sup> )	2	2	2
Temperature (°C)	25	25	45
Substrate material	Copper plates (25x25x0.3mm <sup>l</sup> ) Copper plates (5.0x0.4x0.25mm <sup>l</sup> )		

\*: Sn(II) methanesulfonate

\*\*: Cu(II) methanesulfonate

\*\*\*: Methanesulfonic acid

### 2.3 Observation of Whiskers and Nodules

Whiskers and nodules were observed by SEM. To examine the root of whiskers and nodules, specimens were bent to 180 degree to produce cracks of the deposits as illustrated in *Fig. 1*. The fractured sections at the cracks where whiskers or nodules were expected to exist were observed by SEM.



*Fig. 1 Preparation of specimens for observation of the fractured section of the deposits.*

### 2.4 Determination of Crystal Orientation and Grain Size at the Root of Nodules

The specimens were polished with colloidal silica whose particle size was 0.04μm to smoothen the surface and to reveal the roots of nodules as shown in *Fig. 2*. The crystal orientation and the grains at the roots of nodules were examined by electron backscatter diffraction pattern method (EBSP) with a field emission scanning electron microscope (FESEM).

In this paper, “lateral direction” means the direction parallel to the substrate and “z-axis direction” means the direction perpendicular to the substrate as illustrated in *Fig. 2*.

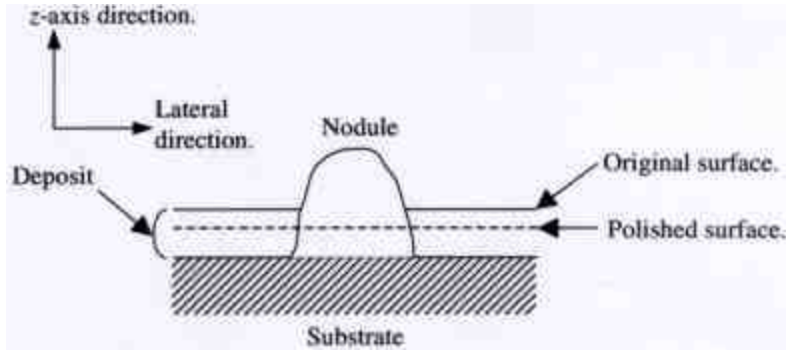


Fig. 2 Preparation of the specimen for EBSD.  
The polished surface of the specimen was analyzed.

### 3. Results and Discussion

#### 3.1 Estimation of Grain-boundary-free Energy

Fig. 3 shows the grains of matt Sn of various thicknesses. Apparently the grain sizes increase with increasing thickness. Matt Sn-0.5%Cu shows the same tendency as matt Sn. Here note that extremely small grains appear in the thin deposits.

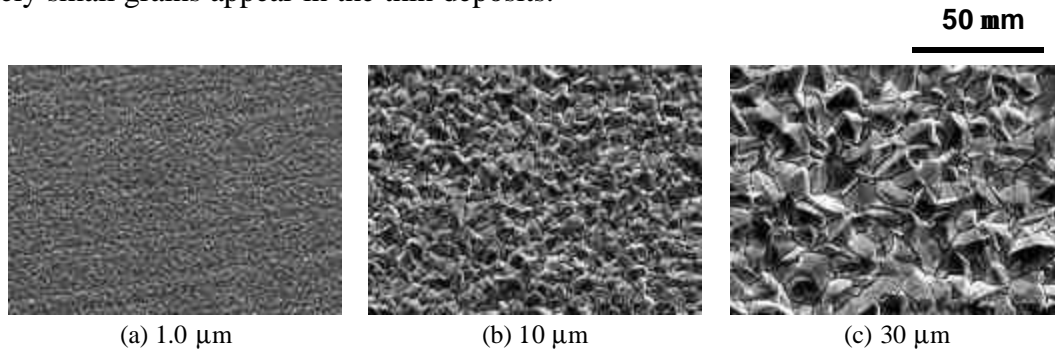


Fig. 3 SEM images of grains of matt Sn of various thickness  $t$ .

In Fig. 4, the average grain sizes  $d$  of matt Sn, bright Sn and matt Sn-0.5%Cu are plotted against square root of the thickness  $t$ . As seen in this figure, matt Sn and matt Sn-0.5%Cu showed good linearity. Then, for matt deposits this relation can be written by

$$d = k\sqrt{t} \quad (\text{Eq. 1})$$

where  $k$  is a constant depending on plating conditions. The obtained values of  $k$  are  $1.57 \mu\text{m}^{1/2}$  for matt Sn and  $1.06 \mu\text{m}^{1/2}$  for matt Sn-0.5%Cu. Regarding matt Sn,  $k$  varied from 1.5 to  $2.0 \mu\text{m}^{1/2}$  depending on the  $\text{Sn}^{2+}$  concentration and the current density. Conversely, the average grain size of bright Sn is found to be independent of the thickness. Then, for bright deposits,  $d$  can be written by

$$d = k' \quad (\text{Eq. 2})$$

where  $k'$  is a constant. For bright Sn,  $k'$  was found to be  $0.56 \mu\text{m}$ .

The difference in these tendencies between matt and bright deposits may be due to the difference in growth mechanism of the deposits. According to A. N. Kolmogorov<sup>16</sup>, *Eq. 1* holds in the case of polycrystalline growth, which is known as “geometrical selection” as schematically illustrated in *Fig. 5*. In the figure, arrows mean the preferential growth directions of each grain. Here let  $\mathbf{q}$  be the angle between the preferential growth direction and the  $z$ -axis direction. If  $\mathbf{q}$  of a grain is large, then the growth of the grain by electrodeposition will be obstructed by a neighboring grain whose  $\mathbf{q}$  is small. Therefore the grains having small  $\mathbf{q}$  can survive and continue to grow dominantly. Hence the number of survived grains gradually decreases with increasing thickness, consequently those grain sizes become larger.

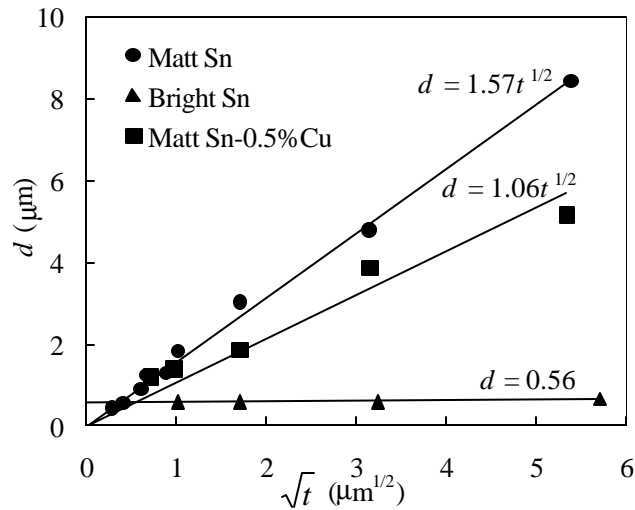


Fig. 4 Relation between average grain size  $d$  and square root of thickness  $t$ .

In the case of matt deposits, it is supposed that geometrical selection may take place in their growth process because *Eq. 1* holds. Meanwhile, for bright deposits, the grain growth in electrodeposition is strongly prohibited by adsorption of additives. Therefore the deposits grow by continuous nucleation predominantly, and then the grain sizes remain small and constant throughout the whole thickness of the deposits.

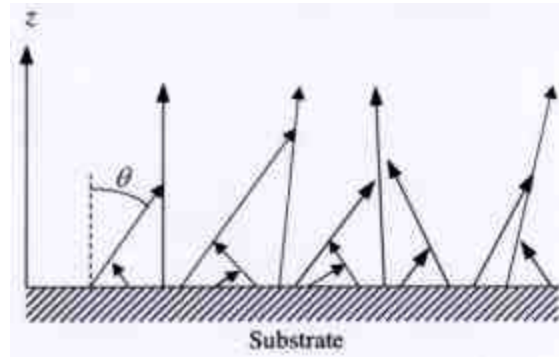


Fig. 5 Schematic explanation of geometrical selection. Arrows mean the preferential growth directions of each grain. Let  $\theta$  be the angle between the preferential growth direction and the  $z$ -axis direction. If  $\theta$  of a grain is large, then the growth of the grain will be obstructed by a neighboring grain whose  $\theta$  is small. Therefore the grains having small  $\theta$  can survive and continue to grow dominantly.

Here, in order to estimate the grain-boundary-free energy per unit volume,  $G_b$ , the grains are assumed to be regular hexagons, which can tessellate the whole surface of a plane, as shown in Fig. 6 (a), and let the length of their side be  $a$ . Consider the grain boundaries on a plane P whose area is  $A$ , and the plane is parallel to the substrate and located at the distance  $z$  from the substrate, as shown in Fig. 6 (b). Then the area of a grain is  $3\sqrt{3} \cdot a^2 / 2$ . Two neighboring grains share a side of the hexagons. Therefore the circumference per grain is  $3a$ , and the number of grains on the plane P is  $2A / (3\sqrt{3} \cdot a^2)$ . Hence the total length of the grain boundaries on the plane becomes  $2A / (\sqrt{3} \cdot a)$ .

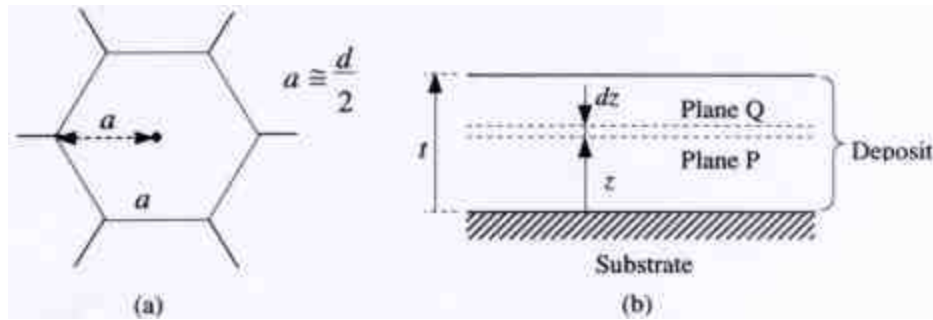


Fig. 6 Regular hexagon model for a grain, (a), and cross section of a deposit, (b).

Here let us consider the small segment between the plane P and a plane Q shown in Fig. 6 (b). The plane Q is located at a small distance  $dz$  from the plane P. The area of the grain boundaries involved in the small segment is given by  $(2A / \sqrt{3} \cdot a) \cdot dz$ . Then the total grain-boundary-free energy involved in this segment can be expressed by  $(2A s_b / \sqrt{3} \cdot a) \cdot dz$ , where  $s_b$  is the grain-boundary-free energy per unit area. Hence the grain-boundary-free energy per unit volume for matt deposits,  $G_b^M$ , can be formulated by

$$G_b^M = \frac{2\mathbf{s}_b}{\sqrt{3} \cdot a}. \quad (\text{Eq. 3})$$

For bright deposits, because the grain sizes remains constant throughout the whole thickness, the bright deposits can be regarded as a layered structure whose each layer is assumed to be tessellated with hexagonal prisms. Therefore the grain boundaries parallel to the substrate should be taken into account. Assuming the height of the hexagonal prism to be  $2a$ , the grain-boundary-free energy of such boundaries per unit volume is given by  $\mathbf{s}_b/2a$ . Then the total grain-boundary-free energy per unit volume for bright deposits,  $G_b^B$ , can be expressed by

$$G_b^B = \frac{(4 + \sqrt{3}) \cdot \mathbf{s}_b}{2\sqrt{3} \cdot a}. \quad (\text{Eq. 4})$$

Meanwhile  $a$  equals to  $d/2$  approximately. Then from Eqs. 1 and 3,  $G_b^M$  at the distance  $z$  from the substrate can be given by

$$G_b^M = \frac{4\mathbf{s}_b}{\sqrt{3} \cdot k\sqrt{z}} = \frac{2.31\mathbf{s}_b}{k\sqrt{z}}. \quad (\text{Eq. 5})$$

From Eqs. 2 and 4,  $G_b^B$  for bright deposits can be written by

$$G_b^B = \frac{(4 + \sqrt{3}) \cdot \mathbf{s}_b}{\sqrt{3} \cdot k'} = \frac{3.31\mathbf{s}_b}{k'}. \quad (\text{Eq. 6})$$

In Eq. 5, if  $z$  approaches to 0, then  $G_b^M$  becomes infinity. However, at the initial stage of electrodeposition, it may begin with nucleation even in the case of matt deposits. After the nuclei have tessellated the whole surface of the substrate, subsequent grain growth in electrodeposition can take place. Therefore the thickness less than the size of a nucleus is needless to consider.

As we discuss later, it is substantially important for whisker and nodule growth whether recrystallization can take place in the deposits. Next, we discuss on the possibility of the occurrence of recrystallization. According to K. T. Aust et al. <sup>17</sup>, the grain-boundary-free energy of tin was determined to be approximately 0.1 J/m<sup>2</sup> at 220 °C. We can use this value at room temperature assuming the temperature dependence of the grain-boundary-free energy is negligible <sup>18</sup> and also applicable for Sn-0.5%Cu. Fig. 7 shows  $G_b$  distribution along  $z$ -axis direction of deposits calculated by Eqs. 5 and 6. In the case of matt deposits,  $G_b$  increases steeply when the distance  $z$  is less than 2 μm. On the other hand, bright deposits show constant  $G_b$  independent of the distance  $z$ . It is said that grain growth as a stage of recrystallization requires 10<sup>4</sup> to 6x10<sup>5</sup> J/m<sup>3</sup> for driving force <sup>19</sup>. Furthermore it is said that recrystallization can take place at the temperature higher than approximately  $T_m/2$ , where  $T_m$  is the melting point in absolute temperature. In the case of tin,  $T_m/2$  is 252.5 K (-20.5 °C). Therefore not only bright deposits but also matt deposits have sufficient free energy to initiate recrystallization at room temperature. If the grain sizes are sufficiently small even in the case of matt deposits, then recrystallization can take place without existence of strain energy. Of course, if there exists strain energy in the deposits, it can also leads to recrystallization.



It is reported that reflowing or annealing of tin deposits can effectively prevent the whisker growth<sup>20</sup>. It can be understood that such treatment make the grain sizes sufficiently large, and then the grain-boundary-free energy will be reduced significantly. However the grain growth by annealing is recrystallization process itself. If recrystallization is directly related to the whisker growth, it seems to be a contradiction because annealing prevents the whisker growth. As we discuss this later, whiskers cannot be formed at elevated temperature even though recrystallization develops more rapidly as compared with room temperature.

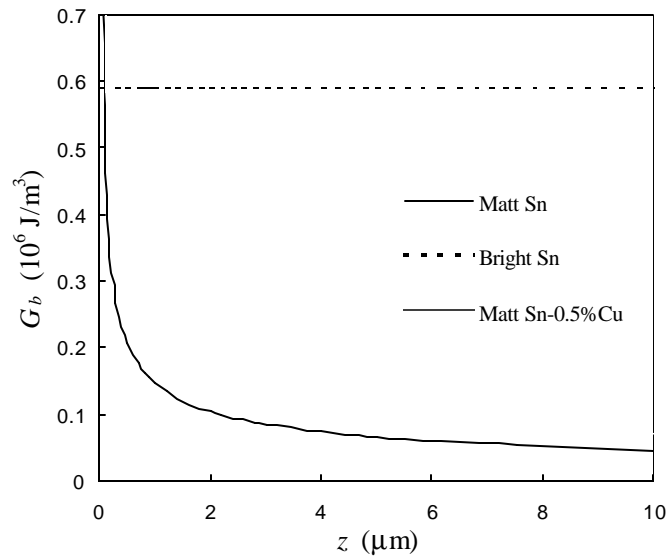


Fig. 7 Grain-boundary-free energy per unit volume,  $G_b$ , distribution along  $z$ -axis direction of deposits.

Fig. 8 shows the crystal orientation of each grain for matt Sn-0.5%Cu, stored at room temperature for 314 days, analyzed by EBSP. Original thickness of the deposits was 4.0  $\mu\text{m}$ , and EBSP analysis was conducted after polishing 0.5  $\mu\text{m}$  from its original surface. The sites of nodules designated as A to E on the SEM image, (a), correspond to the sites designated as the same symbols on the inverse pole figure map, (b). In Fig. 8 (b), black spots are intermetallic compound between tin and copper, which was verified by energy dispersion X-ray (EDX) analysis, and other color-coded segments are all tin grains. As seen in this figure, recrystallized grains are developing underneath the nodules encroaching surrounding small grains. This suggests that a nodule itself may be a recrystallized single crystal of tin. The nodules B and E show approximately the same orientation as that of the matrix. On the contrary, the nodules A, C, and D show different orientation from those. From these crystal orientations of nodules, it does not seem to exist specific growth direction in nodule formation.

Recrystallization itself cannot be the cause of mass-extrusion, i.e. the whisker or the nodule growth, because it can develop only in the lateral direction encroaching the surrounding grains.



To extrude mass from the surface of deposits, tin atoms should flow from the surrounding regions to the roots of nodules by diffusion due to mass-balance. The chemical potential of tin atoms in the recrystallized grain is expected to be considerably smaller than that of unrecrystallized grains because grain-boundary-free energy and also possible strain energy are decreased in the recrystallized grain. Therefore this diffusion process will be driven by this chemical potential difference of tin atoms. The diffusion path may be the interface between the deposits and the substrate. Furthermore, in the case of thin deposits, the extrusion of the recrystallized grain will be more advantageous in surface-free energy than the lateral grain growth without mass-extrusion because the surface area of the grain in the former case will be less than that in the latter case. On the contrary, in the case of substantially thick deposits, the grain growth by recrystallization will take place within the inside of the deposits without mass-extrusion. It is reported that the whisker growth can be reduced when the deposits are thick <sup>7, 20</sup>. This may be related to the lower possibility of mass-extrusion in the case of thick deposits.

The grain growth as a stage of recrystallization is a relaxation process of the grain-boundary-free energy. However another relaxation process should be considered, i.e. the formation of intermetallic compound (IMC) at the interface. It is reported that the whisker growth tends to be strongly affected by the kind of substrate materials <sup>20, 21</sup>. If the grain-boundary-free energy can be relaxed predominantly by IMC formation, whisker growth will be reduced significantly especially in the case of matt deposits.

As shown in *Fig. 8 (b)*, the grain growth in the lateral direction seems to be interfered by surrounding IMC particles although several IMC particles are included in the grains of nodules. As mentioned previously, copper accelerates the whisker growth. We found larger number of whiskers and also nodules on matt Sn-0.5%Cu as compared with matt Sn. If the IMC particles interfere the grain growth in the lateral direction on the way of growth, the grain will be facilitated to extrude from the surface of the deposits. Therefore some impurities, such as copper, accelerate the formation of nodules and subsequently whiskers.

W. C. Ellis et al. <sup>11</sup> and N. Furuta et al. <sup>12</sup> proposed that whiskers were formed directly by recrystallization introducing the immobile and stable grain boundary of a grain, which acts as the nucleus of a whisker. However, from the above facts and discussion, recrystallization process can only lead to the formation of nodules. To form whiskers, another stage of progress should be taken into consideration.

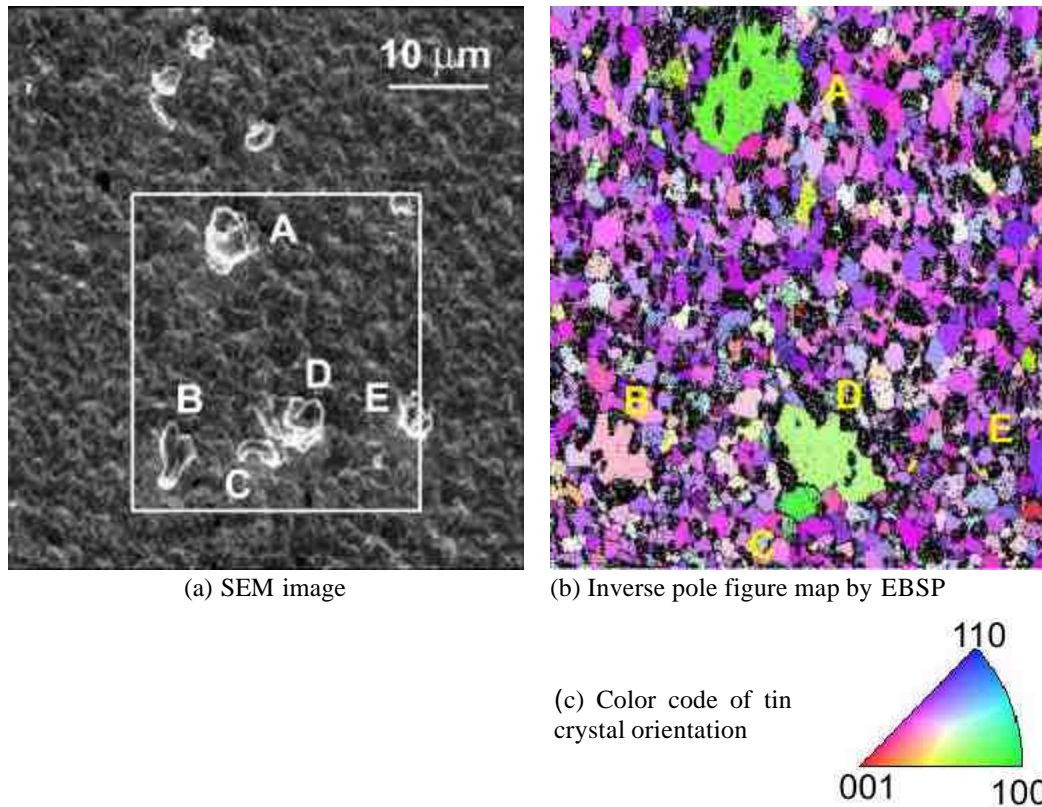


*Fig. 8 Crystal orientation of each grain of matt Sn-0.5%Cu analyzed by EBSD. The electrodeposited specimen was stored at room temperature for 314 days. Original thickness of the deposit was 4.0 mm, and EBSD analysis was conducted after polishing 0.5 mm from its original surface.*

### 3.2 Relation between Nodules and Whiskers

*Fig. 9* shows an example of a whisker that grew on a nodule formed on bright Sn. Regarding bright Sn, almost all whiskers were found to grow on nodules. Generally the shapes of the nodules formed on bright deposits are extremely complicated. While, in the case of matt Sn and Sn-0.5%Cu, it was found that whiskers were growing not only on nodules, *Fig. 10*, but also directly on the deposits, *Fig. 11*. Several nodules designated as A to D can be seen in *Fig. 10* (a), and they seem to represent early stages of the whisker growth on nodules. Among them, the nodules A and B indicate the earliest forms of mass-extrusion followed by the nodules C and D. It can be seen that these nodules have whisker-like filamentary structures (whisker-embryos) on the tops of them, which may formed at the earliest stage of mass-extrusion. These whisker-embryos are expected to grow up to be long whiskers. In *Fig. 10* (b), extremely planar surfaces can be seen at the whisker-embryo. These planar surfaces may be low index planes, so-called facets in terms of crystallography. It is important to understand the meanings why these facets are produced, as we discuss this later.

In the case of directly growing whiskers on the deposits as seen in *Fig. 11* (a), at the tip of the whisker, a granular object can be seen. It seems to be a grain, which was located at the original

surface of the deposit. Therefore this type of whiskers may be initiated to grow from the inside of the deposits, probably from the vicinity of interface because there exists considerable amount of grain-boundary-free energy as shown in *Fig. 7*. It is supposed that this type of whisker growth may be related to the recrystallization process hidden in the deposits. Hence it is suggested that the whisker growth is closely related to the nodule growth, to be precise, to the grain growth stage of recrystallization.

There exists another important feature of whiskers, typically shown in *Figs. 11 (a) and (b)*. When the whisker is thinner, (a), its lateral surface is simple and consists of only a few facets. On the contrary, when it is thicker, (b), its lateral surface becomes complicated and consists of many facets. If the diameter of a whisker becomes thinner, it will be required to be a simpler form to reduce its surface-free energy further more because its surface area becomes larger as compared with its volume. This means the morphology of the microstructure, such as whiskers, depends closely on the tendency to lower the surface-free energy.

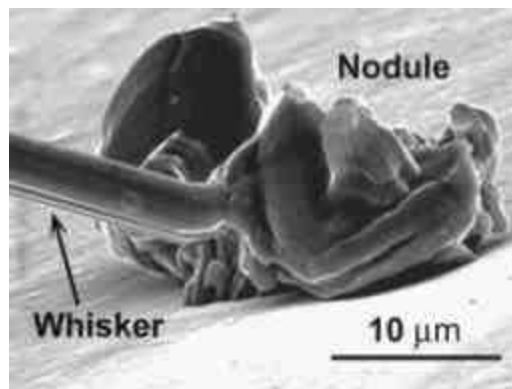
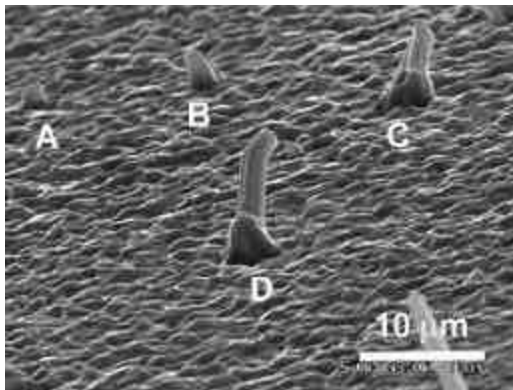
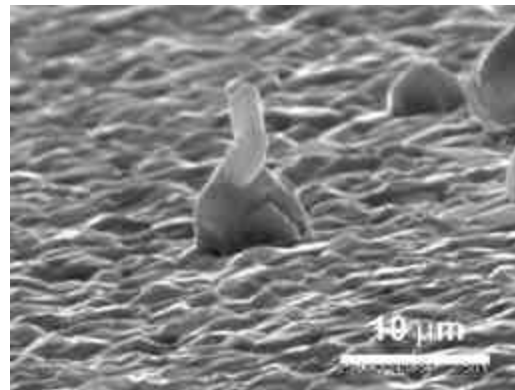


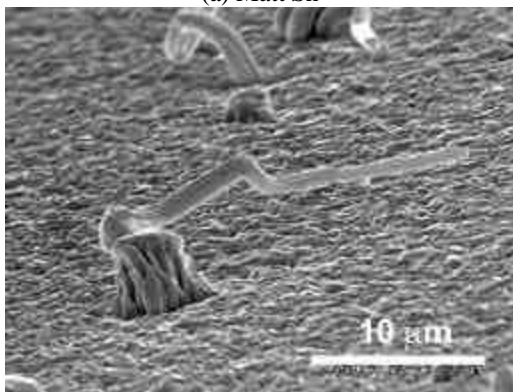
*Fig. 9 An example of a whisker growing on a nodule. The specimen was plated with 4.34  $\mu\text{m}$  of bright Sn, and stored at room temperature for 680 days.*



(a) Matt Sn

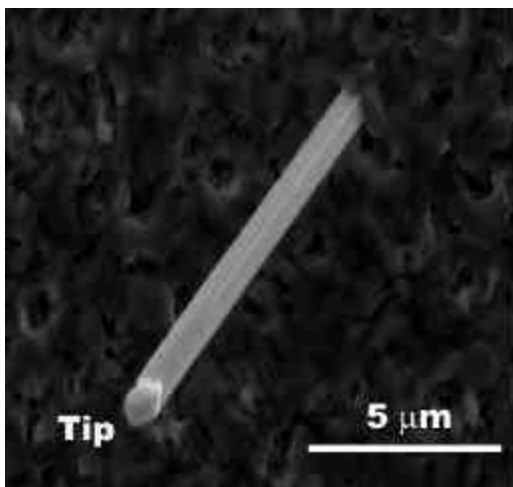


(b) Matt Sn

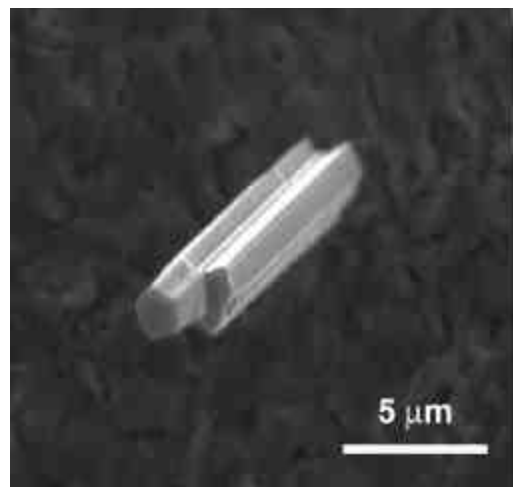


(c) Matt Sn-0.5%Cu

*Fig. 10 Examples of whiskers growing on nodules formed on (a) 1.85 **mm** of matt Sn, which was stored at room temperature for 751 days, (b) 3.96 **mm** of matt Sn-0.5%Cu stored at room temperature for 732 days.*

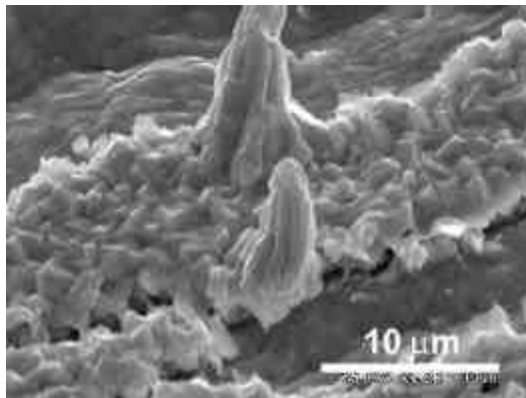


(a)

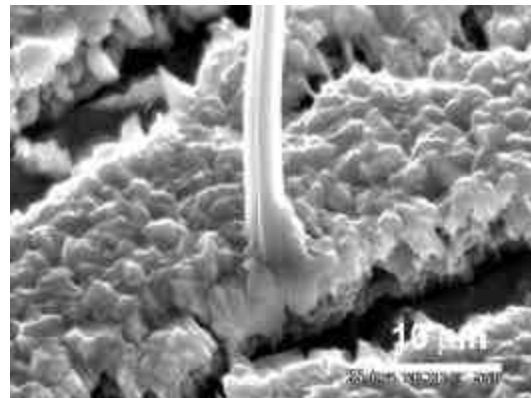


(b)

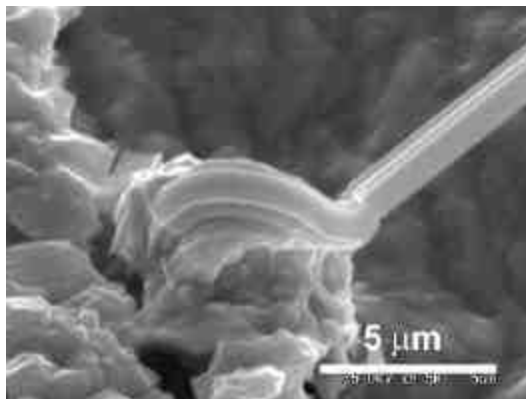
*Fig. 11 Examples of whiskers growing directly on 6.03 **mm** of matt Sn-0.5%Cu stored at room temperature for 66 days.*



(a) Fractured section of a nodule.



(b) Fractured section of a whisker.



(c) Fractured section of a whisker.

*Fig. 12 Fractured sections of a nodule, (a), and whiskers, (b) and (c), formed on 4.45  $\mu\text{m}$  of matt Sn-0.5%Cu stored at room temperature for 689 days.*

*Fig. 12* shows the fractured sections of a nodule, (a), and whiskers, (b) and (c). From *Fig. 12* (a), the nodule seems to grow from the interface between the deposit and the substrate. This seems to support that the nodules were formed by the grain growth accompanied with the interfacial diffusion of tin atoms as discussed previously. As seen in *Figs. 12* (b) and (c), nodules are found at the roots of the whiskers. These nodules also seem to grow from the vicinity of interface. Any whiskers growing without nodules were not found in this investigation. These facts support the close relation between nodules and whiskers.

Whiskers and nodules can be distinguished by their morphology and surface condition. The shapes of nodules are very irregular and complicated and their surfaces are substantially rough and consist of general surface (not specific surface such as facets). While typical whiskers are surrounded by regular and smooth facets on their lateral surfaces. From this, it is suggested that whiskers may grow on nodules as a result of the tendency of reducing surface-free energy of nodules. In other words, the driving force for the formation of whiskers from nodules is supposed to be the surface-free energy difference between whiskers and nodules. In this case, strain energy cannot be the driving force because nodules are already recrystallized structures.



### 3.3 Whisker Formation Process

Fig. 13 shows a whisker growing on a nodule formed on bright Sn. To be precise, it is not a typical whisker because its diameter is not constant. This type of whiskers can be often seen in bright deposits. From A to D, designated in the figure, this whisker may consist of one or two single crystals because there may exist a possible grain boundary at C. The segment, from A to B, may be formed by general nodule growth process. It seems that this segment was originally located on another nodule, such as segment E. However the residual segment, from B to D, may be formed by different growth mechanism. At the present, a grain boundary exists at D, which separates the nodule and the whisker (N/W boundary). It is supposed that this N/W boundary might have been migrating from B to D in the past continuously creating new configurations of tin atoms. Therefore the shapes of the N/W boundary in the past are recorded on the lateral surface of this whisker. It can be seen that the lateral surface becomes gradually smoother to reduce the surface-free energy as the diameter of this whisker becomes smaller. In this case, the force reducing the diameter of the whisker may be the grain boundary tension, equivalent to grain-boundary-free energy, at the N/W boundary, and the driving force for the migration of the N/W boundary is supposed to be the surface-free energy difference between the nodule and the whisker.

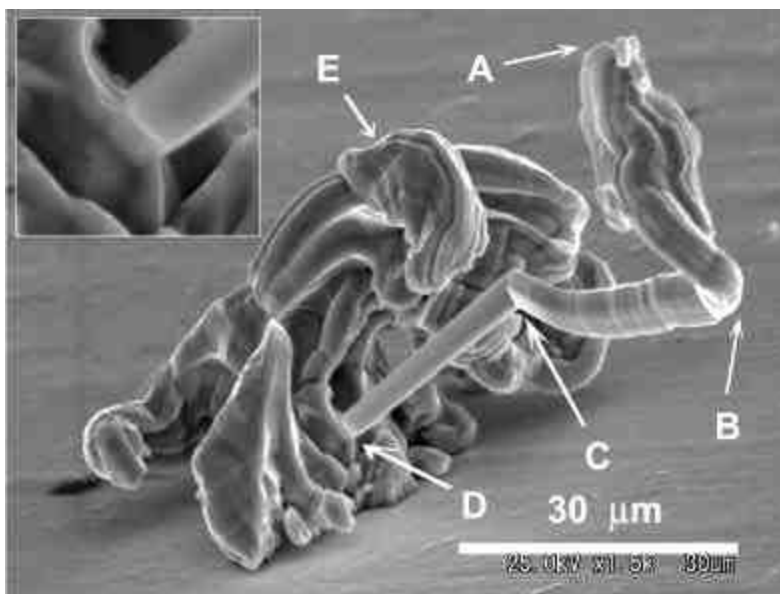
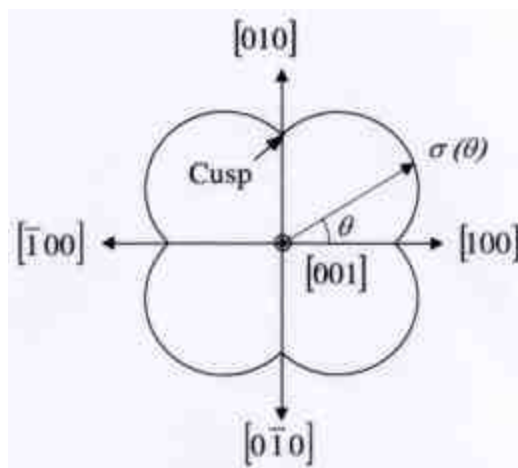


Fig. 13 A whisker growing on a nodule. The specimen was plated with 4.34  $\mu\text{m}$  of bright Sn stored at room temperature for 664 days.

If this whisker continues to reduce its diameter still further, then it will be forced to create facets on the lateral surface. In the case of *Fig. 13*, facets have not been created. However, it should be mentioned, the growth process of this type of whiskers suggest the possibility that the migration of the N/W boundary driven by surface-free energy difference may lead to create facets on the lateral surfaces of whiskers. There may be another possible way for creating facets. In a certain atmosphere and at certain temperature range, the surface of certain metals tends to decompose to produce facets and rather complex index planes in order to reduce total surface-free energy, and this phenomenon is known as “faceting”<sup>13, 23</sup>. The facets, which can be seen in *Fig. 10 (b)* on a whisker-embryo, may be formed by such faceting.

Generally facets have cusped minima in surface-free energy<sup>13, 22</sup>. *Fig. 14* explains schematically such cusped minima, e.g. {100} planes, in the case of tin. The facets are stable in terms of stiffness due to such nature of the surface-free energy. It means that the whiskers whose lateral surfaces consist of facets can grow only in the direction maintaining the planes of the facets themselves. This can explain the reason why the cross sectional shapes of whiskers remains unchanged throughout almost whole length.



*Fig. 14 Schematic diagram of the surface-free energy  $\sigma(\theta)$  of  $b$  tin in the direction perpendicular to  $[001]$  axis.*

*The surface-free energy  $\sigma(\theta)$  is a function of angle  $\theta$ .  
Cusped minima can be seen in  $\langle 100 \rangle$  directions.*

It is reported that the growth direction of tin whiskers is limited to several directions, i.e.  $\langle 001 \rangle$ ,  $\langle 100 \rangle$ ,  $\langle 101 \rangle$  and  $\langle 111 \rangle$ <sup>1, 2</sup>. W. C. Ellis<sup>1</sup> considered this fact related to the slip directions in plastic deformation of tin single crystal. However  $\langle 100 \rangle$  direction is not included in such slip directions<sup>24</sup>. There should be different meanings of the directions. It must be emphasized that these directions have zone planes, listed in Table 2, whose surface-free energy is expected to be in cusped minima. The zone planes are parallel to each growth direction; therefore they can compose the lateral surfaces of the whisker in the form of facets. It should be noted that minimization of surface-free energy can be achieved by growing in those specific directions.



Table 2 Growth directions of tin whiskers and their zone planes.

Growth direction of tin whisker.	Zone planes.
$\langle 001 \rangle$	$\{100\}, \{210\}, \{110\}$
$\langle 100 \rangle$	$\{001\}, \{101\}, \{301\}, \{100\}$
$\langle 101 \rangle$	$\{100\}, \{411\}, \{211\}, \{101\}$
$\langle 111 \rangle$	$\{110\}, \{321\}, \{211\}, \{312\}, \{101\}, \{112\}$

When the temperature is elevated near the melting point of the metal, the cusped minima in surface-free energy will become shallow because the entropy term of the free energy cannot be negligible at elevated temperature. Therefore facets cannot maintain their stability at such temperature because of so-called “thermal roughening”. *Fig. 15* shows the shapes of whiskers formed at 100 °C. It can be seen that the lateral surfaces of the whiskers are not planar any longer and extinguish their stability. This experimental result supports the above expectation. Here we can conclude that the stable filamentary shapes of whiskers are due to the stability of the facets created on their lateral surfaces.

#### 4. Conclusion

It has been shown that the grain-boundary-free energy is sufficient for spontaneous occurrence of recrystallization of the layer, especially in the case of thin layers because of their extremely small grains. While many whiskers were found to grow on nodules, this means the whisker growth is closely related to the nodule growth. From these facts, it has been suggested that the nodule formation can be explained by recrystallization, and the whisker growth can be understood as a result of minimization of the surface-free energy of nodules, which have large surface-free energy as a result of their complicated surfaces. Furthermore it has been suggested that the minimization of the surface-free energy can be achieved growing in the specific directions and creating facets on the lateral surface. From this, some important nature of whiskers, e.g. the growth directions and the stability of the cross sectional shapes, and temperature dependence on growth can be understood.

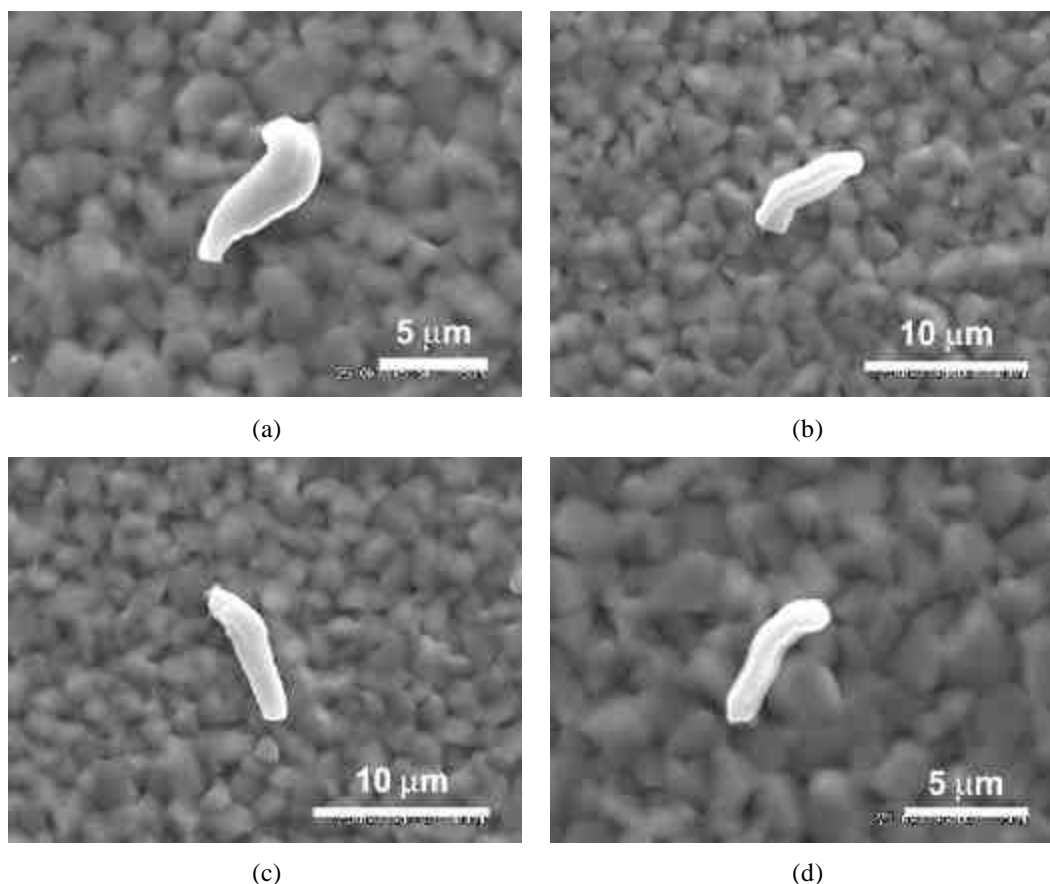


Fig. 15 Whiskers formed at 100°C.  
The specimen was plated with 1.96  $\mu\text{m}$  of matt Sn  
and stored at 100°C for 48 hours.

## Reference

1. W.C. Ellis, *Trans. Met. Soc. AIME*, **236**, 872 (1966).
2. H.G. Smith & R.E. Rundle, *J. App. Phys.*, **29**, 679 (1958).
3. C. Herring & J.K. Galt, *Phys. Rev.*, **85**, 1060 (1952).
4. S.C. Lawrence, *Bull. Am. Phys. Soc., Ser. II*, **3**, 328 (1958).
5. U. Lindborg, *Met. Trans. A*, **6A**, 1581 (1975).
6. K.N. Tu, *Acta Met.*, **21**, 347 (1973).
7. B.Z. Lee & D.N. Lee, *Acta Mater.*, **46**, 3701 (1998).
8. J.D. Eshelby, *Phys. Rev.*, **91**, 755 (1953).
9. F.C. Frank, *Phil. Mag.*, **44**, 854 (1953).
10. U. Lindborg, *Acta Met.*, **24**, 181 (1976).
11. W.C. Ellis, D.F. Gibbons & R.G. Treuting, *Growth and Perfection of Crystals*, John Wiley, New York, 1958; p. 102.
12. N. Furuta & K. Hamamura, *Jap. J. App. Phys.*, **8**, 1404 (1969).

13. C. Herring, *Phys. Rev.*, **82**, 87 (1951).
14. V.K. Glaznova & K.M. Gorbunova, *J. Crystal Growth*, **10**, 85 (1971).
15. M.E. Williams, C.E. Johnson, K-W. Moon, G.R. Stafford, C. A. Handwerken & W. J. Boettinger, *Proc. AESF SUR/FIN 2002*, p. 148 (2002).
16. A.N. Kolmogorov, *Dokl. Acad. Nauk SSSR*, **65**, 681 (1949).
17. K.T. Aust & B. Chalmers, *Proc. Roy. Soc.*, **A204**, 359 (1951).
18. W.R. Tyson, *Can. Metall. Q.*, **14**, 307 (1975).
19. F.J. Humphreys & M. Hatherly, *Recrystallization and Related Annealing Phenomena*, Elsevier Science Ltd, Oxford, U.K., 2002; p.9.
20. S.C. Britton, *Trans. Inst. Met. Fin.*, **52**, 95 (1974).
21. K. Whitlaw & J. Crosby, *Proc. AESF SUR/FIN 2002*, p. 136 (2002).
22. N.A. Gjostein, *Acta Met.*, **11**, 957 (1963).
23. N.A. Gjostein, *Acta Met.*, **11**, 969 (1963).
24. C.S. Barrett, *Structure of Metals*, McGraw Hill, New York, 1952; p. 337.